8-1-2022

Does Sea Spray Aerosol Contribute Significantly To Aerosol Trace Element Loading? A Case Study From the U.S. GEOTRACES Pacific Meridional Transect (GP15)

Chris M. Marsay
University of Georgia, christopher.marsay@skio.uga.edu

William M. Landing
Florida State University, wlanding@fsu.edu

Devon Umstead
University of Georgia

Claire P. Till
Humboldt State University

Robert Freiberger
Humboldt State University

See next page for additional authors

Global Biogeochemical Cycles®

RESEARCH ARTICLE
10.1029/2022GB007416

Special Section:
The U.S. GEOTRACES Pacific Meridional Transect (GP15)

Does Sea Spray Aerosol Contribute Significantly to Aerosol Trace Element Loading? A Case Study From the U.S. GEOTRACES Pacific Meridional Transect (GP15)

Chris M. Marsay[1], William M. Landing[2], Devon Umstead[1], Claire P. Till[3], Robert Freiberger[3,4], Jessica N. Fitzsimmons[5], Nathan T. Lanning[5], Alan M. Shiller[6], Mariko Hatta[7,8], Rebecca Chmiel[9], Mak Saito[9], and Clifton S. Buck[1]

[1]Skidaway Institute of Oceanography, University of Georgia, Savannah, GA, USA, [2]Department of Earth, Ocean and Atmospheric Science, Florida State University, Tallahassee, FL, USA, [3]Department of Chemistry, Humboldt State University, Arcata, CA, USA, [4]Now at Scripps Institution of Oceanography, University of California San Diego, La Jolla, CA, USA, [5]Department of Oceanography, Texas A&M University, College Station, TX, USA, [6]Division of Marine Science, University of Southern Mississippi, Stennis Space Center, Hattiesburg, MS, USA, [7]Department of Oceanography, University of Hawai'i at Mānoa, Honolulu, HI, USA, [8]Institute of Arctic Climate and Environmental Research, Japan Agency for Marine-Earth Science and Technology, Yokosuka, Japan, [9]Marine Chemistry and Geochemistry Department, Woods Hole Oceanographic Institution, Woods Hole, MA, USA

Abstract Atmospheric deposition represents a major input for micronutrient trace elements (TEs) to the surface ocean and is often quantified indirectly through measurements of aerosol TE concentrations. Sea spray aerosol (SSA) dominates aerosol mass concentration over much of the global ocean, but few studies have assessed its contribution to aerosol TE loading, which could result in overestimates of "new" TE inputs. Low-mineral aerosol concentrations measured during the U.S. GEOTRACES Pacific Meridional Transect (GP15; 152°W, 56°N to 20°S), along with concurrent towfish sampling of surface seawater, provided an opportunity to investigate this aspect of TE biogeochemical cycling. Central Pacific Ocean surface seawater Al, V, Mn, Fe, Co, Ni, Cu, Zn, and Pb concentrations were combined with aerosol Na data to calculate a "recycled" SSA contribution to aerosol TE loading. Only vanadium was calculated to have a SSA contribution averaging >1% along the transect (mean of 1.5%). We derive scaling factors from previous studies on TE enrichments in the sea surface microlayer and in freshly produced SSA to assess the broader potential for SSA contributions to aerosol TE loading. Maximum applied scaling factors suggest that SSA could contribute significantly to the aerosol loading of some elements (notably V, Cu, and Pb), while for others (e.g., Fe and Al), SSA contributions largely remained <1%. Our study highlights that a lack of focused measurements of TEs in SSA limits our ability to quantify this component of marine aerosol loading and the associated potential for overestimating new TE inputs from atmospheric deposition.

Plain Language Summary Sea spray aerosol (SSA) generated by breaking waves and bursting bubbles can dominate the particle population in the marine atmosphere. We investigated whether this mechanism could mobilize significant amounts of trace elements (TEs)—nutrient and pollutant elements present in the surface ocean in very low concentrations. Previous studies have suggested that TEs could become enriched on SSA during its formation, relative to their concentrations in seawater, and this could make the process a more significant source for aerosol concentrations of some elements. But for others, the SSA contribution is always likely to be insignificant. Our calculations based on sea salt and TE aerosol concentrations in the atmosphere and dissolved TEs in the surface ocean suggest that SSA does not contribute significantly to total aerosol TE loading, with the possible exception of vanadium, which has relatively higher concentrations in seawater than the other elements considered. This study highlights that this process remains poorly quantified due to limited direct measurements.

Key Points:

- Sea spray aerosol (SSA) concentration was quantified along a meridional Pacific Ocean transect during low mineral aerosol conditions
- Sea spray-derived aerosol trace elements (TEs) are negligible unless significant enrichment occurs during formation; only vanadium is >1%
- SSA contributions to aerosol TEs of >100% calculated by applying enrichments from earlier studies suggests these are not widely applicable

Supporting Information:

Supporting Information may be found in the online version of this article.

Correspondence to:

C. S. Buck and C. M. Marsay,
csbuck@uga.edu;
christopher.marsay@skio.uga.edu

Citation:

Marsay, C. M., Landing, W. M., Umstead, D., Till, C. P., Freiberger, R., Fitzsimmons, J. N., et al. (2022). Does sea spray aerosol contribute significantly to aerosol trace element loading? A case study from the U.S. GEOTRACES Pacific Meridional Transect (GP15). *Global Biogeochemical Cycles*, *36*, e2022GB007416. https://doi.org/10.1029/2022GB007416

Received 14 APR 2022
Accepted 16 JUL 2022

Author Contributions:

Conceptualization: Chris M. Marsay, William M. Landing
Data curation: Chris M. Marsay, Devon Umstead, Claire P. Till, Robert Freiberger, Jessica N. Fitzsimmons, Nathan T.

1. Introduction

Aerosols originating from natural and anthropogenic sources play multiple important roles in the global climate system, including direct radiative forcing through scattering or absorption of solar radiation, through acting as cloud condensation nuclei, and through their redistribution of nutrients and pollutants by long-range atmospheric transport and deposition (Boucher et al., 2013). This latter facet can lead to aerosols impacting biogeochemical

Lanning, Alan M. Shiller, Mariko Hatta, Rebecca Chmiel, Mak Saito, Clifton S. Buck
Formal analysis: Chris M. Marsay
Funding acquisition: William M. Landing, Claire P. Till, Jessica N. Fitzsimmons, Alan M. Shiller, Mariko Hatta, Mak Saito, Clifton S. Buck
Investigation: Chris M. Marsay
Methodology: Chris M. Marsay, Claire P. Till, Jessica N. Fitzsimmons, Alan M. Shiller, Mariko Hatta, Mak Saito, Clifton S. Buck
Project Administration: William M. Landing, Claire P. Till, Jessica N. Fitzsimmons, Alan M. Shiller, Mariko Hatta, Mak Saito, Clifton S. Buck
Resources: Chris M. Marsay, William M. Landing, Devon Umstead, Claire P. Till, Robert Freiberger, Jessica N. Fitzsimmons, Nathan T. Lanning, Alan M. Shiller, Mariko Hatta, Rebecca Chmiel, Mak Saito, Clifton S. Buck
Supervision: William M. Landing, Clifton S. Buck
Validation: Chris M. Marsay, William M. Landing, Devon Umstead, Claire P. Till, Robert Freiberger, Jessica N. Fitzsimmons, Nathan T. Lanning, Alan M. Shiller, Mariko Hatta, Rebecca Chmiel, Mak Saito, Clifton S. Buck
Visualization: Chris M. Marsay
Writing – original draft: Chris M. Marsay
Writing – review & editing: Chris M. Marsay, William M. Landing, Devon Umstead, Claire P. Till, Robert Freiberger, Jessica N. Fitzsimmons, Nathan T. Lanning, Alan M. Shiller, Mariko Hatta, Rebecca Chmiel, Mak Saito, Clifton S. Buck

cycles and ecosystems at a great distance from their emission regions (Hamilton et al., 2020; Mahowald et al., 2005, 2017; Shaw, 1995).

Mineral aerosol (dust) is the major aerosol component responsible for atmospheric transport of iron (Fe) and several other trace elements (TEs), including aluminum (Al), titanium (Ti), manganese (Mn), and cobalt (Co) (Jickells et al., 2005; Mahowald et al., 2009, 2018), following mobilization from arid continental regions during wind events (Kaufman et al., 2005; Merrill et al., 1989; Prospero et al., 2002; Zhang et al., 1997). Volcanic eruptions and wind erosion of glacial till also introduce mineral aerosol to the atmosphere (Achterberg et al., 2013; Langmann et al., 2010; Prospero et al., 2012). Subsequent atmospheric deposition is an important TE delivery mechanism to the surface ocean, where the rate of supply can influence primary production and phytoplankton community structure (C. M. Moore et al., 2013; Jickells et al., 2005; J. K. Moore et al., 2004; Martin et al., 1990). For several elements with lower concentrations in lithogenic material, including vanadium (V), nickel (Ni), copper (Cu), zinc (Zn), and lead (Pb), anthropogenic emissions and biomass burning are more important sources for atmospheric delivery to the oceans (Mahowald et al., 2018; Pacyna et al., 2016). Furthermore, despite the lower content of Fe in combustion emissions, there is evidence that these aerosols nevertheless significantly contribute to the atmospheric deposition of soluble Fe (Desboeufs et al., 2005; Ito et al., 2019; Pinedo-González et al., 2020; Sholkovitz et al., 2009).

Despite the importance of dust and anthropogenic emissions for atmospheric transport of nutrients and pollutants, the aerosol mass concentration in the marine atmosphere is often dominated by sea spray aerosol (SSA; Arimoto et al., 1995; Boucher et al., 2013; Duce et al., 1980; Prospero, 1979), an estimated $2–100 \times 10^{15}$ g per year of which is emitted from the ocean surface (de Leeuw et al., 2011). SSA is formed by the bursting of bubbles at the sea surface, following their entrainment in the upper water column by breaking waves and at higher wind speeds, by the tearing of wave crests (Blanchard, 1989; de Leeuw et al., 2011). This sea-to-air mass flux is dominated by inorganic sea salt, particularly for the larger particles produced, but numerous laboratory and field studies have also shown a significant organic fraction, particularly in submicrometer size aerosols, while microorganisms can also be emitted during bubble bursting (Aller et al., 2005; Blanchard & Syzdek, 1970; Cavalli et al., 2004; O'Dowd et al., 2004; Prather et al., 2013).

The potential for sea-to-air transport of TEs during the production of SSA, either as a "recycled" input by resuspension of previously deposited aerosols, or as a source of "new" aerosol TEs, remains understudied. A handful of studies have indicated that this contribution may amount to a small but significant percentage for TEs, including Al, V, Fe, Cu, and Zn (Arimoto et al., 2003; Cattell & Scott, 1978; Weisel, Duce, Fasching, et al., 1984). A significant sea spray contribution to total aerosol TE loading would result in overestimates of new atmospheric delivery to the surface ocean if overlooked in measurements of aerosol TE concentrations or deposition fluxes. As a result, the topic is worthy of investigation as part of multidisciplinary community research projects, such as GEOTRACES and the Surface Ocean Lower Atmosphere Study.

However, such measurements are complicated by the difficulty of separating aerosol TEs associated with SSA versus dust and other aerosol types. A handful of previous studies have attempted to do so by using purpose-built equipment to sample an isolated parcel of near-ocean atmosphere while simulating SSA formation (Pattenden et al., 1981; Piotrowicz et al., 1979; Weisel, Duce, Fasching, et al., 1984) or by using radioactive isotope tracers (van Grieken et al., 1974).

In this paper, we make use of the low dust concentrations measured during the U.S. GEOTRACES Pacific Meridional Transect to investigate this facet of TE biogeochemistry. We use concurrent measurements of aerosol and surface ocean TE concentrations to estimate the minimum contribution of SSA to aerosol TE loading, assuming that there is no TE enrichment relative to surface seawater composition during sea spray formation. In addition, we use data from previous studies on TE enrichments in the sea surface microlayer and from studies focusing on freshly produced SSA to estimate the maximum SSA contribution to TE aerosol loading.

2. Methods

2.1. Sample Collection

Sampling was conducted on board the R/V Roger Revelle as part of the U.S. GEOTRACES GP15 Pacific Meridional Transect (henceforth GP15) during September–November 2018. After an initial southeasterly transit

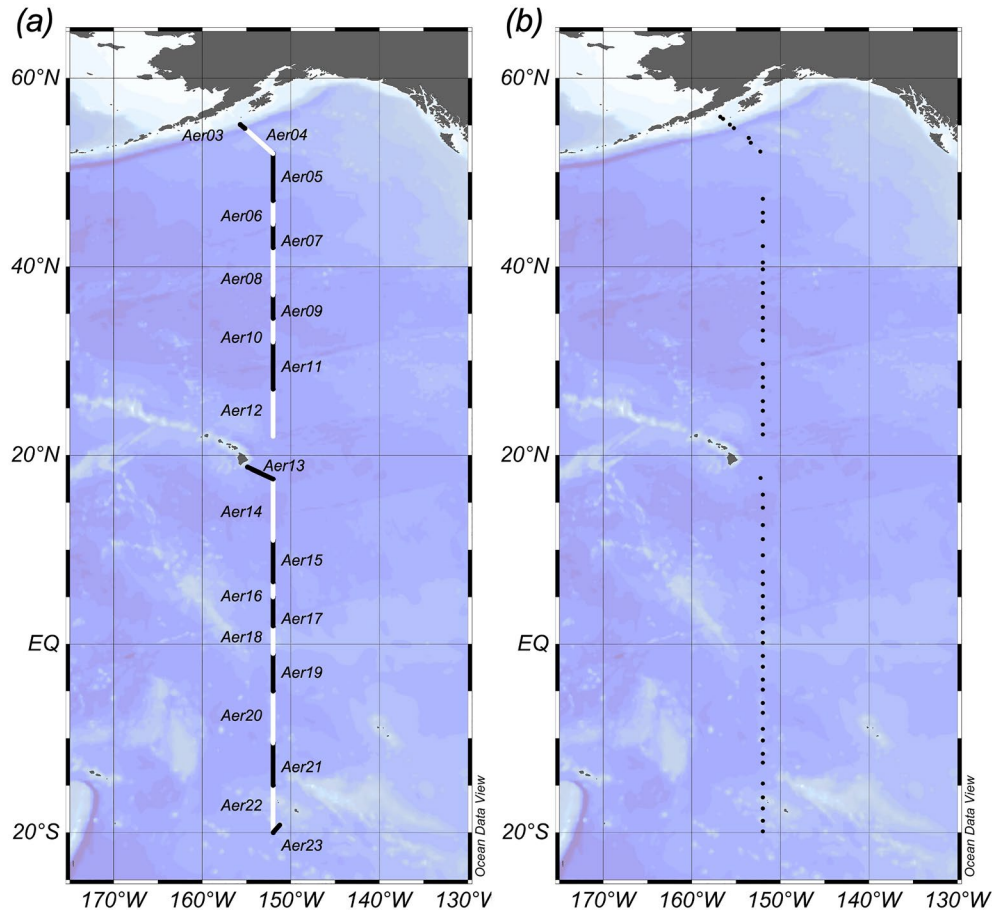

Figure 1. Map of the study area for the U.S. GEOTRACES GP15 transect with (a) aerosol deployments represented by black (odd deployments) or white (even deployments) lines spanning from deployment to recovery positions and (b) towfish sampling locations, represented by black dots.

offshore from the Alaskan shelf, GP15 followed a north-south transect along the 152°W meridian between 52°N and 20°S, before ending at Papeete, Tahiti on 24 November (Figure 1). The transect was carried out over two legs (RR1814 and RR1815) with a personnel exchange in Hilo, Hawaii (21–24 October).

Aerosol sample collection, including full details of individual deployments, has been described in Marsay et al. (2022) and was consistent with protocols from previous U.S. GEOTRACES cruises. Briefly, bulk aerosol samples were collected over 1–4 days using high-volume aerosol samplers (~1.2 m^3 air min^{-1}; Tisch Environmental, model 5170V-BL) deployed on the forward rail of the ship's 03 deck, approximately 16 m above sea level. Sampling was sector-controlled to avoid contamination from the ship's stack exhaust, and filters (47 mm diameter; Whatman 41) were acid-washed before use to reduce TE blanks. After recovery, filters for bulk TE analyses were transferred to petri slides and stored frozen until processing ashore, while separate replicate filters were leached with ultrapure water at sea (details below).

Surface seawater sampling was carried out using a towfish deployed from the starboard side of the vessel at a depth of ~3 m (Bruland et al., 2005) with seawater pumped through Teflon tubing from the fish into a clean "bubble" set up onboard. Filtered samples (0.2 µm AcroPak) were taken while underway just before arrival at each hydrostation and occasionally during transit approximately halfway between stations (Figure 1). Sampling into acid-cleaned plastic bottles was conducted following GEOTRACES protocols (Cutter et al., 2017) before distribution of samples to the various groups measuring specific TEs.

2.2. Sample Processing and Analysis

Treatment and analysis of filters for aerosol TE measurements are described in full in Marsay et al. (2022). Briefly, triplicate filters from each deployment were digested with concentrated nitric and hydrofluoric acids and hydrogen peroxide and the residues redissolved in 0.32 M double-distilled HNO_3 for the analysis of Al, Ti, V, Mn, Fe, Co, Ni, Cu, Zn, and Pb by inductively coupled plasma mass spectrometry (ICP-MS; Perkin Elmer NexION 300D), using a seaFAST S2 system (Elemental Scientific Inc.; ESI) without preconcentration. Measured TE concentrations were blank corrected by subtracting the mean digestion blank for unused filters, then normalized to pmol/m^3 by dividing by the volume of air sampled. All bulk aerosol TE concentrations used in this paper are archived at the Biological and Chemical Oceanography Data Management Office (BCO-DMO; Buck et al., 2021a, 2021b).

Additional filters from each deployment were treated at sea with a rapid flow-through leach using 100 mL of ultrahigh purity (UHP) water (Buck et al., 2006) with an acid-washed 0.2 µm polycarbonate backing filter (Whatman Nuclepore) installed on the filter rig behind each sample filter. A 5 mL subsample from each leach was stored frozen until the return to shore, then thawed in a refrigerator before being analyzed for major ions by ion chromatography (Dionex ICS-2100). Concentrations of major cations (Na^+, Ca^{2+}, Mg^{2+}, and K^+) and anions (Cl^-, NO_3^-, and SO_4^{2-}) were determined against external standards prepared with ACS grade salts (Fisher). Aerosol major ions data are available through BCO-DMO but only the $Na+^+$ data are presented here (Buck et al., 2022a, 2022b). The Na^+ data were generated using a Dionex IonPac CS12 chromatography column (4 × 250 mm) at 40°C. The eluent was 20 mM methanesulfonic acid.

For shipboard determination of dissolved Al, filtered samples were drawn into acid-washed 125 mL polymethylpentene bottles and analyzed within 24 hr of collection. Samples were acidified to 0.006 M HCl using subboiling distilled HCl and were microwaved in groups of four for 3 min at 900 W to 60 ± 10°C. Samples were allowed to cool for at least 1 hr prior to analysis of Al by Flow Injection Analysis (FIA), using methods of Resing and Measures (1994). FIA results, normally reported in nM units, have been converted to nmol/kg by dividing by the density of seawater at 20°C and its measured salinity. These data are archived at BCO-DMO (Hatta & Measures, 2022a, 2022b).

Samples for dissolved Co were collected and stored in acid-washed low-density polyethylene (LDPE) bottles (Nalgene) at 4°C prior to analysis. Analysis was carried out by cathodic stripping voltammetry, following an established 1h UV oxidation procedure (Chmiel et al., 2022; Hawco et al., 2016; M. A. Saito & Moffett, 2001). All data are archived at BCO-DMO (M. A. Saito, 2021; M. Saito, 2020).

Surface seawater samples for analyses of dissolved Mn, Ni, and Pb were collected in LDPE bottles, acidified to 0.024 M HCl (Fisher Optima) and analyzed using the methods of Biller and Bruland (2012), with adaptations as described in Parker et al. (2016). Briefly, this method involves preconcentration of the metals onto Nobias Chelate PA-1 resin (Sohrin et al., 2008). Seawater is buffered to pH 6.0 ± 0.2 just before loading onto the resin columns and eluted with 1 M HNO_3 (Fisher Optima). Seawater extracts were analyzed on a sector field ICP-MS (Thermo Scientific Element XR) and calibrated with standard addition curves made in low-metal seawater. Data used in this study are archived at BCO-DMO (Freiburger et al., 2022a, 2022b).

Subsamples for dissolved Fe, Cu, and Zn analyses were collected in LDPE bottles, acidified to 0.024 M HCl (Fisher Optima), and analyzed using a seaFAST system (ESI) following the methods of Lagerström et al. (2013), as updated in Jensen et al. (2020). This method involves a 25× preconcentration of metals onto Nobias Chelate PA-1 resin after they are spiked with a solution enriched in ^{57}Fe, ^{65}Cu, and ^{68}Zn and buffered inline to pH 6.2 ± 0.2. The metals are back-eluted into 1.6 M HNO_3 (Fisher Optima) and quantified using isotope dilution after analysis on a Thermo Scientific Element XR ICP-MS. Figures of merit for this method can be found in Jensen et al. (2020) and all the data used are found in Table S1.

Dissolved V analyses followed the isotope dilution method of Ho et al. (2018). Briefly, acidified 14 mL subsamples (0.024 M HCl; Fisher Optima) taken from high-density polyethylene bottles were spiked with a ^{50}V-enriched solution (44.3% ^{50}V; Oak Ridge National Laboratories) and extracted/preconcentrated into 1 mL of eluate (1.6 M HNO_3; Seastar Baseline) using a seaFAST system with Nobias Chelate PA-1 resin (Biller & Bruland, 2012; Sohrin et al., 2008). A similar online seaFAST extraction procedure is described by Hathorne et al. (2012) for rare earth elements. Eluates from the seaFAST system were analyzed by Thermo Scientific Element XR ICP-MS

Table 1
Summary (Range, Mean ± 1σ) of Aerosol Trace Element, Na, Dust, and Sea Salt Concentrations During U.S. GEOTRACES GP15, and the Mean (±1σ) Percentage Lithogenic Contribution to Total Aerosol Trace Element and Na Concentrations

	Concentration range	Concentration mean ± 1σ	Lithogenic contribution (%; mean ± 1σ)
		pmol/m^3	
Al	104–645	296 ± 162	77 ± 38
Ti	1.2–18	5.0 ± 4.5	100
V	0.10–7.6	2.1 ± 2.4	11 ± 11
Mn	0.3–3.3	1.1 ± 0.8	81 ± 33
Fe	11–146	52 ± 38	94 ± 42
Co	0.026–0.124	0.066 ± 0.026	19 ± 10
Ni	0.39–2.5	1.2 ± 0.7	2.3 ± 1.3
Cu	0.36–9.3	2.0 ± 2.2	2.7 ± 2.5
Zn	2.1–18.7	7.1 ± 3.9	1.5 ± 1.3
Pb	0.03–3.82	0.41 ± 0.80	4.1 ± 2.3
		nmol/m^3	
Na	33–379	126 ± 80	0.10 ± 0.10
		ng/m^3	
Dust[a]	18–283	80 ± 72	–
Sea salt[b]	2,448–28,353	9,439 ± 5,965	–

Note. Lithogenic contributions are calculated based on the aerosol Ti concentration and the average element/Ti ratio of the upper continental crust composition (Taylor & McLennan, 1995). Ti is 100% by definition.

[a]Dust concentrations calculated from Ti data and assuming all Ti is from crustal material with an average 0.3% Ti content by weight (Taylor & McLennan, 1995). [b]Sea salt concentration calculated from Na data and assuming all Na is from sea salt with an average 30.7% Na content by mass (Prospero, 2002).

operated in medium resolution and using a PC3 sample introduction system (ESI) to obtain the intensities of ^{50}V and ^{51}V. Additionally, ^{47}Ti and ^{52}Cr were monitored to correct for any ^{50}Ti or ^{50}Cr isobaric interference on ^{50}V; the correction was generally <1%. Figures of merit for this method can be found in Ho et al. (2018) and the data are found in Table S1.

3. Results

3.1. Aerosol Trace Element Concentrations

Aerosol TE and Na concentrations during GP15 are summarized (range and mean ± one standard deviation [1σ]) in Table 1. The transect took place outside of the usual springtime peak in North Pacific aerosol concentrations associated with eastward transport of mineral aerosol and industrial emissions from Asia (Hsu et al., 2008; Merrill et al., 1989; Parrington et al., 1983). Consequently, measured aerosol TE concentrations were some of the lowest reported from GEOTRACES studies, particularly for elements typically dominated by mineral aerosol concentrations (Marsay et al., 2022). Mineral aerosol concentrations, calculated from Ti data and assuming an average upper continental crustal (UCC) Ti content of 0.3% (Taylor & McLennan, 1995), ranged from 18 to 283 ng/m^3 and are presented in Figure 2. Using aerosol Al and an average UCC Al content of 8.04% gives a similar range (35–216 ng/m^3). Estimates of the mineral aerosol contribution to aerosol loading for each TE were calculated based on Ti data and average UCC ratios from Taylor and McLennan (1995) and are summarized in Table 1.

Soluble Na concentrations in GP15 aerosols spanned 33–379 nmol/m^3 (Table 1). Assuming that all measured soluble Na are derived from sea salt with an average 30.7% Na contribution by mass (Prospero, 2002), we calculate sea salt concentrations (as an approximation of SSA) during GP15 of 2,448–28,353 ng/m^3 (mean of 9,439 ng/m^3). Thus, SSA loading was between 24× and 1,026× (median 149×) greater than mineral aerosol loading in samples collected throughout the GP15 section (Figure 2). These calculations assume that none of the Na associated with mineral aerosol is extracted into the soluble phase by the UHP water leach. However, we also calculated a theoretical mineral aerosol contribution to Na (Na_{lith}), based on the Ti concentration (which is assumed to be completely crustal in origin) and the average Na/Ti ratio of crustal material (Taylor & McLennan, 1995), $(Na/Ti)_{lith}$, such that:

$$Na_{lith} = Ti \times (Na/Ti)_{lith} \quad (1)$$

Given the relatively low-mineral aerosol concentrations encountered during GP15, this calculation indicates that dust would have contributed ∼0.1% of the measured Na on average (maximum 0.4%), and thus, no lithogenic corrections were applied to the Na data.

3.2. Surface Seawater Trace Element Concentrations

Concentrations of dissolved TEs measured in a total of 54 surface seawater samples collected by towfish are summarized in Table 2 (range and mean ± 1σ) along with salinity. For some elements, fewer than 54 data points are available due to subsamples not being collected or to occasional data points not meeting quality control verification. Spatial variations in dissolved TE concentrations are not discussed here as they will be addressed in future papers focused on water column TE distributions.

For each towfish sample, the Na concentration was also calculated based on the salinity measurement (Guildline Autosal salinometer) of a dedicated subsample and by normalizing to a seawater Na concentration of 469 mmol/kg

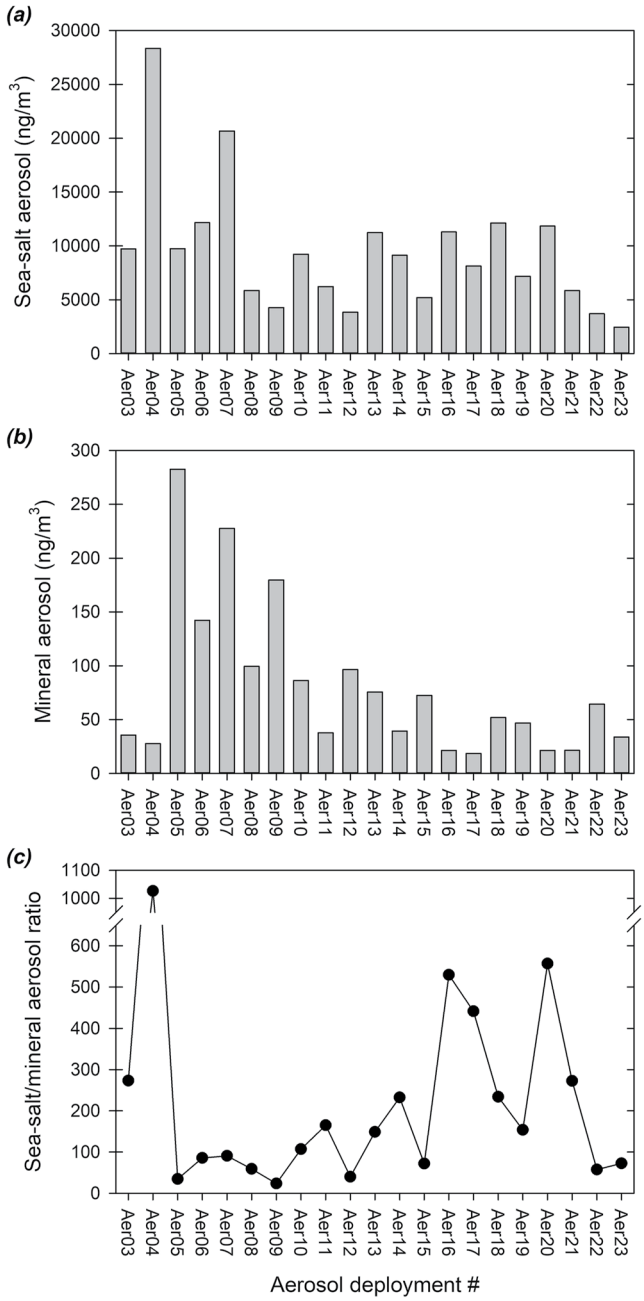

Figure 2. Concentrations of (a) sea salt aerosol and (b) mineral aerosol for GP15 aerosol deployments Aer03–Aer23, calculated from aerosol Na and Ti concentrations, respectively (see text for details). Note different concentration scales. Also shown is (c) the mass ratio of sea salt to mineral aerosol for each sample. Note break in *y*-axis.

at salinity 35 (Pilson, 2013). From the calculated Na and dissolved TE concentrations, the TE/Na molar ratio was calculated for each towfish sample. Mean ($\pm 1\sigma$) TE/Na values across the GP15 section are summarized in Table 3.

4. Discussion

Previous studies have suggested that in remote ocean regions with low-mineral aerosol loading, SSA can contribute significantly to aerosol concentrations of some TEs (Arimoto et al., 2003; Duce et al., 1983; Weisel, Duce, Fasching, et al., 1984). Given the wide disparity in dust and sea salt concentrations during GP15 and the small contributions to many of our measured TEs from lithogenic materials (with the exceptions of Al, Ti, Mn, and Fe; Table 1), we investigated whether TEs associated with sea salt could contribute significantly to the totals measured during GP15.

Our initial calculations relate aerosol data directly to measured concentrations of dissolved TEs in surface seawater based on the assumptions that TE/Na ratios in SSA are representative of those in bulk surface seawater within the sampling region and that only dissolved phase TEs are incorporated during aerosol production. However, neither of these assumptions are necessarily representative of SSA production. Numerous studies have demonstrated small but significant fractionation of major cations in SSA, relative to seawater, and larger enrichments of organic material, along with the incorporation of marine particulate material into SSA (Aller et al., 2005; Duce & Hoffman, 1976; Jayarathne et al., 2016; Keene et al., 2007; Quinn et al., 2014). Such enrichments have been associated with the scavenging of surface-active material from the upper ocean by bubbles as they rise to the sea surface and with the fact that those bubbles pass through the sea surface microlayer, itself an environment distinct from bulk seawater, before they burst to produce SSA (Aller et al., 2005; Jayarathne et al., 2016; Robinson et al., 2019).

Few studies have tried to measure TE enrichment directly in naturally produced SSA. Weisel, Duce, Fasching, et al. (1984) used a Bubble Interfacial Microlayer Sampler (BIMS) in the Sargasso Sea to measure TE concentrations in SSA derived from purposefully generated bubbles. They calculated enrichment factors (EFs) for Al, Sc, V, Mn, Fe, Co, Cu, Zn, and Pb in these aerosols relative to surface seawater and sodium concentration, such that:

$$EF = {}^{(TE/Na)_{aer}}/_{(TE/Na)_{sw}} \quad (2)$$

where $(TE/Na)_{aer}$ is the ratio of a TE to Na in BIMS-generated aerosols and $(TE/Na)_{sw}$ is their ratio in surface seawater. From the Sargasso Sea sampling, Weisel et al. reported EF values as high as 20,000 for some elements.

Based on these aspects of SSA production, we therefore also use data from the Weisel et al. study along with an assessment of the relative concentrations of dissolved and particulate TEs in surface waters and data from studies quantifying TE enrichment in the surface microlayer. From these evaluations, we quantify potential scaling factors that should be applied to bulk surface seawater dissolved TE concentrations to estimate TE incorporation into SSA. We then apply these scaling factors to the GP15 data to assess potential SSA contributions to aerosol TE loading.

Table 2
Summary of Dissolved Trace Element Concentrations and Salinity From Surface Seawater Collected by Towfish Along the GP15 Transect

	Concentration range	Concentration mean ± 1σ	Number of samples
	nmol/kg		
Al	0.5–8.6	2.3 ± 2.1	48
V	27.7–33.8	30.9 ± 1.5	54
Mn	0.45–7.39	0.99 ± 0.99	54
Fe	0.06–0.48	0.19 ± 0.11	46
Ni	1.7–6.4	2.7 ± 0.9	54
Cu	0.39–3.54	0.81 ± 0.60	54
Zn	0.03–0.71	0.12 ± 0.11	50
	pmol/kg		
Co	<DL[a]–562	12 ± 21[b]	33
Pb	2–52	23 ± 10	54
Salinity	31.4–36.3	34.4 ± 1.3	54

[a]Some Co concentrations below method detection limit (<DL) of 1.7 pmol/kg. [b]Excludes two high Co concentrations from Station 1 (562 pmol/kg) and Station 2 (239 pmol/kg). For 10 samples with Co < DL, a concentration equal to the 1.7 pmol/kg DL is used.

4.1. Sea Spray Aerosol Contributions Based on Towfish-Dissolved TE Concentrations

Due to the specific sampling strategies used during GP15, towfish and aerosol sample collections did not correspond directly (Figure 1), while it is likely that not all SSA collected during any one aerosol sampling originated within that specific area of sample collection. Thus, seawater TE/Na ratios were averaged from any towfish samples collected within ±1° latitude of the deployment span of each aerosol sample and then combined with Na data from that aerosol sample to calculate a theoretical SSA contribution to the TE concentration (in pmol/m^3). For each sample, these concentrations were then expressed as a percentage of the total aerosol concentration of each element.

Except for V, SSA TE contributions calculated without any scaling factors applied averaged <0.1% for all elements considered (Table 3), with the maximum contribution of each (always <1%) calculated for Aer04, which had the highest soluble Na concentration (Figure 2). The calculated SSA contribution for V averaged 1.5 ± 1.8% (median: 1.1%) along the GP15 section (Figure 3). In the North Pacific (samples Aer03–Aer12), where mineral aerosol loading was higher and oil combustion emissions are thought to have had a strong influence on aerosol V loading (Marsay et al., 2022), the SSA contribution averaged (±1σ) 0.32 ± 0.29%, with the highest contribution of 1.1% for Aer04, as for other measured TEs. However, the lower loading of total aerosol V in the equatorial Pacific (Aer13–Aer23) combined with the relatively high concentration of V in seawater resulted in a higher calculated SSA contribution to V during Leg 2 with an average of 2.7 ± 1.9% and a maximum contribution of 7.1% (Aer16).

4.2. Incorporation of Particulate TEs Into Sea Spray Aerosol and Implications

Bubbles are capable of transporting particulate materials as they rise through the surface ocean (Wallace & Duce, 1975), and this material can be transported across the sea-air interface as evinced by the presence of intact and fragmented bacteria and phytoplankton in SSA (Aller et al., 2005; Blanchard, 1989; Blanchard & Syzdek, 1970; Guasco et al., 2014; Patterson et al., 2016).

No particulate TE measurements were made on towfish samples during GP15. However, such measurements were made on towfish samples during the U.S. GEOTRACES GP16 section in the eastern South Pacific, which intersected the southern end of the GP15 transect and took place at the same time of year. Using a combination of dissolved and particulate TE data from each GP16 towfish sample, we calculated an average scaling factor (Table 4) to apply to the GP15 towfish data to account for surface water particles being incorporated into SSA. This average scaling factor increases SSA contributions by less than a factor of 2 for all elements except Fe and Zn (which increase by a factor of 3; Table 4). The highest scaling factor calculated for any GP16 station was 11, for Zn, which would still only result in a maximum SSA contribution to aerosol Zn of <0.2%. Thus, we conclude that accounting for surface ocean particulate TE concentrations would have little effect on our calculated SSA contributions.

Table 3
Mean (±1σ) Dissolved Trace Element (TE)/Na Ratios From GP15 Towfish Samples and the Range and Median (in Parentheses) of Percentage Sea Spray Aerosol (SSA) Contributions to Aerosol TE Load

	Seawater TE/Na (pmol/mmol)	% SSA contribution
Al	5.0 ± 4.6	All <0.001% (2×10^{-4}%)
V	67.1 ± 1.5	0.08%–7.1% (1.1%)
Mn	2.2 ± 2.3	0.003%–0.32% (0.02%)
Fe	0.42 ± 0.24	All <0.001% (1×10^{-4}%)
Co	0.08 ± 0.25	<0.001%–0.128% (0.002%)
Ni	5.9 ± 2.1	0.006%–0.60% (0.05%)
Cu	1.8 ± 1.4	<0.001%–0.421% (0.009%)
Zn	0.27 ± 0.25	<0.001%–0.013% (4×10^{-4}%)
Pb	0.051 ± 0.021	<0.001%–0.022% (0.003%)

Note. % SSA contributions are derived from aerosol Na data and the seawater TE/Na ratio from nearby towfish samples.

4.3. Application of SSA Trace Element Enrichments Determined in the Sargasso Sea

The BIMS study conducted in the Sargasso Sea is one of very few studies that have attempted to measure TEs specifically associated with SSA. The average BIMS-derived EF values from Weisel, Duce, Fasching, et al. (1984)

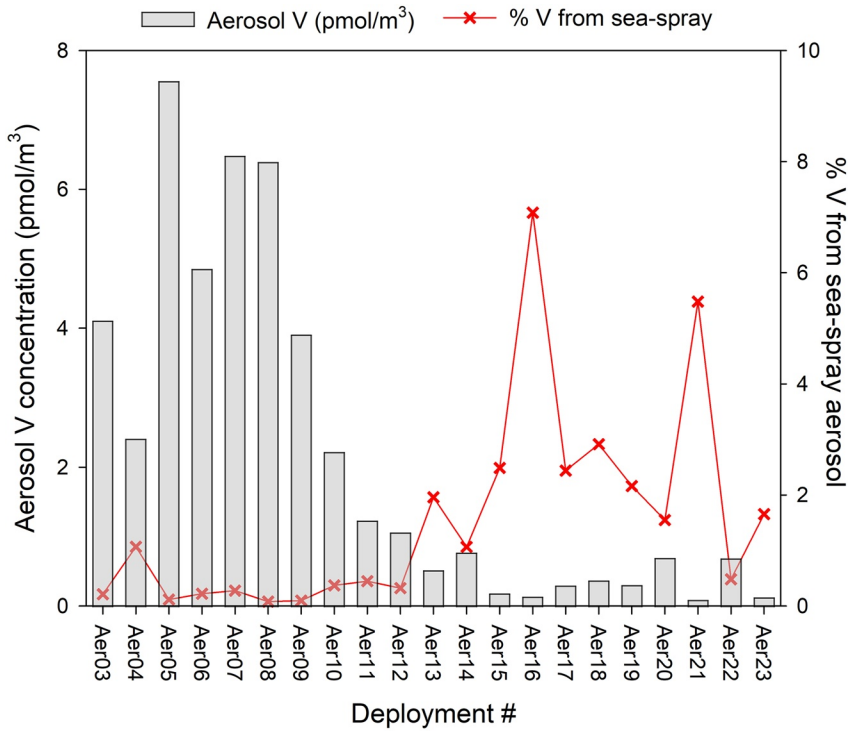

Figure 3. Aerosol V concentrations (Marsay et al., 2022) displayed alongside percentage contributions to aerosol V from sea spray aerosol (calculated as described in the text). Note that the scale bar for the latter only extends to 10%.

are listed here in Table 5. Assuming the Sargasso Sea BIMS data to be representative of the open ocean, we used these EF values with our calculated TE/Na ratios from towfish samples and applied them to the GP15 aerosol Na data. Unsurprisingly, this greatly increased the calculated SSA contributions for some TEs (Figure 4) with median values across all aerosol samples ranging from 0.1% (Co) to 106% (V). However, this approach also gave SSA contributions of >100% in some cases for Zn (1 sample), Cu (2 samples), Mn (3 samples), and V (11 samples, including 10 from Leg 2) (Figure 4). For V and particularly for Mn, this is inconsistent with the low enrichments of these elements relative to crustal material in GP15 aerosol samples. Aerosol Mn/Ti ratios across the section averaged only 1.3 times that of crustal material as indicated by an average ~80% lithogenic contribution to aerosol Mn loading (Table 1). Aerosol V enrichment, relative to crustal material, was lower during Leg 2 than Leg 1 (Marsay et al., 2022), which is inconsistent with the high SSA contributions to Leg 2 aerosol V suggested by applying the BIMS-derived sea spray enrichment for V to Leg 2 data.

These results thus suggest that the enrichments observed in SSA from Sargasso Sea BIMS samples are not directly applicable to Pacific Ocean aerosols and raise the question of their wider applicability beyond the Sargasso Sea region. As previously mentioned, there have been very few studies that have directly addressed potential enrichments of TEs in SSA. However, we note that of the few other previous studies, summarized in Table 5, the enrichments calculated for the Sargasso Sea study are at the high end of estimates for Cu, Fe, Zn, and Pb (Pattenden et al., 1981; Piotrowicz et al., 1979; Weisel, Duce, Fasching, et al., 1984).

An earlier BIMS study in Narragansett Bay by Piotrowicz et al. (1979) determined average EFs for Fe and Zn in SSA of ~80 and ~200, respectively; much lower than 10,000 and 20,000 reported for the Sargasso Sea study. The same study also reported Cu EFs averaging ~200, which are somewhat closer to the value of 800 reported for the Sargasso Sea. However, the Piotrowicz et al. study was also conducted in an estuarine environment, which is distinct from the open ocean in terms of TE loading and biological processes and so not directly comparable. Measurements made using a similar sampling approach in the North Sea by Pattenden et al. (1981) reported EFs of <2–76 for Co (similar to the Weisel et al. average of 60), <50 for Zn, and 100–400 for Pb (both much lower than the Sargasso Sea values). Van Grieken et al. (1974) used a radioactive isotope, ^{65}Zn, to study potential enrichment of Zn in SSA in a series of laboratory experiments and reported EFs of up to ~50, relative

Table 4
Dissolved and Particulate Trace Element (TE) Concentration Ranges From Towfish Samples Collected at Stations 7–36 of the U.S. GEOTRACES Eastern Pacific Zonal Transect and the Resulting Median Scaling Factor (Range in Parentheses) to be Applied to GP15 Dissolved TE Data

	Dissolved TE concentrations (dTE)[a]	Particulate TE concentrations (pTE)[b]	Scaling factor (dTE + pTE)/dTE	
			Median	Range
	nmol/L			
Al	0.65–1.02	0.29–2.32	1.7	(1.3–3.9)
V	31.9–34.7	0.02–0.28	1.00	(1.00–1.01)
Mn	0.51–3.83	0.02–0.06	1.03	(1.01–1.05)
Fe	0.03–0.12	0.14[c]	3.2	(2.2–5.7)
Ni	2.14–3.46	0.02–0.17	1.02	(1.01–1.06)
Cu	0.42–1.36	0.02–0.05	1.04	(1.03–1.06)
Zn	0.01–0.29	0.02–0.10	2.8	(1.1–11.2)
	pmol/L			
Co	3–67	2.0–12.6	1.3	(1.1–2.0)
Pb	12–19	0.29–0.62	1.03	(1.02–1.04)

[a]Dissolved TE data are published in or associated with: Ho et al. (2019) (Al); Ho et al. (2018) (V), Resing et al. (2015) (Mn, Fe); Boiteau et al. (2016) (Ni, Cu); John et al. (2018) (Zn), Hawco et al. (2016) (Co); and Boyle et al. (2020) (Pb). [b]Particulate TE data are from Biological and Chemical Oceanography Data Management Office data set #648543 (Sherrell et al., 2016). [c]Only two particulate Fe concentrations were above the detection limit (both 0.14 nmol/L); this value is used for all stations when calculating the scaling factor.

Table 5
Reported Enrichment Factors for TEs in Studies of Sea Spray Aerosol

	Sargasso Sea[a]	Narragansett Bay[b]	North Sea[c]	Gulf of Mexico[d]
Al	5,000	–	–	–
V	100	–	–	–
Mn	1,000	–	–	–
Fe	10,000	83	–	–
Co	60	–	<2–76	–
Ni	–	–	–	–
Cu	800	210	–	–
Zn	20,000	230	<50	<2–50
Pb	4,000	–	140–410	–

[a]Averaged values, summarized in Table 4 of Weisel, Duce, Fasching, et al. (1984). [b]Averaged values, summarized in Table 1 of Piotrowicz et al. (1979). [c]Range of five samples, summarized in Table 3 of Pattenden et al. (1981). [d]Estimated range shown across size fractions in Figures 7 and 8 of van Grieken et al. (1974).

to unfiltered seawater; again much lower than Zn enrichments reported by Weisel et al., while Walker et al. (1986) reported EFs of 30–600 for the radionuclides Pu and Am in similar experiments.

We suggest some potential explanations for the much higher EFs calculated in the Sargasso Sea study. One is that the collected SSA included "recycled" mineral aerosol that had been scavenged from surface waters by the BIMS-generated bubbles. The study took place in July, which is during the seasonal maximum for episodic Saharan dust transport to the Sargasso Sea and surface waters were likely impacted by the deposition of mineral dust in the preceding days and weeks (Arimoto et al., 1995, 2003). In addition, for Fe and Co, the Sargasso Sea BIMS study compared the aerosol data to seawater TE/Na ratios derived from Pacific Ocean data (Weisel, Duce, Fasching, et al., 1984). For Fe, the seawater concentration used (~1 nM) is significantly lower than the ~5 nM concentrations of total dissolvable Fe that has been measured in surface water Sargasso Sea samples influenced by summertime dust deposition (Sedwick et al., 2005). This, however, would only affect the BIMS-derived Fe EF by a factor of five, which would still suggest an EF of 2000 for Fe. It is also acknowledged in the Sargasso Sea study that the calculated Mn and V enrichments represent maximum values estimated from measurable samples with other samples being indistinguishable from filter blanks (Weisel, Duce, Fasching, et al., 1984). For these reasons, we consider the EFs determined in the Sargasso Sea study to represent maximum scaling factors that could be applied to calculate the contribution of SSA to aerosol TEs.

4.4. Consideration of the Surface Microlayer

Given the lack of corresponding SSA TE data sets outside of the Sargasso Sea BIMS study, we also consider reported enrichments of TEs in surface microlayer samples. The surface microlayer (SML) is an almost ubiquitous thin film (10–100s of μm thickness) at the air-sea interface (Cunliffe et al., 2013). It is physicochemically and biologically distinct from bulk seawater, being enriched in organic molecules (carbohydrates, lipids, and proteins) as well as bacteria and phytoplankton (Cunliffe et al., 2013; Hardy, 1982), which could potentially be the cause of enrichments observed in SSA. Enrichments of surface-active organic material within the SML are thought to originate largely from phytoplankton exudates in the bulk surface ocean, which are scavenged by bubbles as they rise to the surface (Robinson et al., 2019; Wurl et al., 2011).

Given the incorporation of TEs into biogenic material and the complexation of dissolved TEs by certain organic molecules, it may be expected that they too would be enriched in the SML relative to bulk seawater. A handful of studies have indeed measured enrichments of TEs in surface microlayer samples (summarized in Table 6). Although not all samples or elements have shown SML enrichments, the small number of measurements reveals occasional enrichments of up to one or two orders of magnitude across multiple TEs with EFs of several hundred reported for Fe and Pb in the Mediterranean Sea and the North Atlantic, respectively (Tovar-Sánchez et al., 2019, 2020). While SML studies of TEs often measure concentrations of an unfiltered sample and report total TE content, Ebling and Landing (2015) differentiated measurements into dissolved and particulate fractions, demonstrating that the greatest TE enrichment is usually seen in the particulate phase.

Based upon this small number of data sets, it is clear that the SML can be enriched in TEs relative to bulk seawater for both dissolved and particulate fractions. As the SML represents the interface between ocean and atmosphere

Table 6
Reported Surface Microlayer (SML) Enrichment Factors for Trace Elements

Region	Al	V	Mn	Fe	Co	Ni	Cu	Zn	Pb	References
Narragansett Bay	–	–	–	2–28	–	1.8–2	3–4	–	1.2–2	Duce et al. (1972)[a]
Hawaii	–	–	–	4.2	–	–	3.1	2.8	–	Barker and Zeitlin (1972)[b]
Florida Keys	<1–4	<1–2	<1–1.2	<1–3	–	<1–1.3	<1–1.1	<1–6	<1–3	Ebling and Landing (2017)[c]
Mediterranean	–	1–2	–	4–896	8–62	1.1–1.8	1.7–21	4–34	1.2–17	Tovar-Sánchez et al. (2020)[d]
Mediterranean	–	–	–	92	3	2	4	–	139	Tovar-Sánchez et al. (2019)[e]
Antarctic	–	–	–	22	4	1.7	8	–	17	
NE Atlantic 2006	–	–	–	193	20	2	111	–	804	
NE Atlantic 2007	–	–	–	99	17	4	148	–	193	
Arctic	–	–	–	50	6	2	13	–	69	
Mediterranean										Ebling and Landing (2015)[f]
Total	1–4	–	<1–1.2	<1–4	1–1.8	<1–1.9	<1–4	<1–1.9	1.2–1.6	
Dissolved	<1–1.5	–	<1–1.1	<1–3	<1–1.6	<1–2	<1–3	<1–1.8	1.1–1.3	
Particulate	1–14	–	1–5	1–5	1–5	2–3	<1–16	1–6	1–13	

Note. Measurements were made on unfiltered samples or are combined concentrations from different analyzed phases. Some enrichment factors were calculated on paired SML and seawater samples, others used average SML and seawater concentrations from several samples.

[a]Based on combined concentrations from each analyzed fraction in SML and seawater from 20 cm depth (Table 1 of Duce et al., (1972)). [b]Based on reported average concentrations in unfiltered sampled from SML and seawater from 60 cm depth (Table 3 of Barker and Zeitlin (1972)). [c]Based on total concentrations (dissolved + labile and refractory particulate fractions) in SML and seawater from ~30 cm depth over two sampling periods (from data submitted to Biological and Chemical Oceanography Data Management Office). [d]Based on concentrations in unfiltered samples from SML and seawater from ~1 m depth (Table 1 of Tovar-Sánchez et al. (2020)). [e]Based on averaged concentrations for SML and seawater from 1 m depth from multiple unfiltered samples in each region (Table 1 of Tovar-Sánchez et al. (2019)). [f]Dissolved and particulate fractions are shown separately, as well as enrichment factors for total concentrations, based on concentrations in SML and seawater from ~30 cm depth (Table 7 of Ebling and Landing (2015)).

and the last contact between bubbles and seawater before they burst, it is reasonable to expect that these enrichments may be transferred to the SSA. However, the enrichments reported in these few studies cannot account for the much higher EFs reported for SSA collected by the BIMS. One caveat to this comparison is that SML enrichments relative to bulk seawater are calculated based upon an operationally defined microlayer thickness (ranging from 26 to 150 μm in the studies summarized in Table 6). Duce et al. (1972) noted that if the true SML thickness is less than this, the samples being collected will be partially diluted by the inclusion of underlying seawater. They calculate that a true SML thickness of just a few molecular layers (~10 nm) would result in an underestimation of SML enrichment from their samples by a factor of 1.5×10^4; thus, a measured Cu EF of five would actually represent an enrichment of the order of 75,000. Values such as this, however, are even greater than the enrichments reported for SSA by Weisel, Duce, Fasching, et al. (1984).

Another way in which measured SML enrichments may underestimate TE enrichments in SSA is through saturation. Data from the Sargasso Sea BIMS study appeared to show that Zn and Pb became more enriched in SSA for bubbles produced at greater depth, suggesting an ongoing scavenging of these elements as the bubbles rose through the water column (Weisel, Duce, Fasching, et al., 1984). In theory, the bubble surface could therefore become more enriched in these elements than their corresponding enrichment in the SML with this potentially preserved during SSA formation. Such a depth-related dependency of TE enrichment was not observed for elements other than Zn and Pb, though the authors noted that any correlation could be masked by uncertainty in measurements.

4.5. Does Sea Spray Aerosol Contribute Significantly to Aerosol TE Loading During GP15?

Without a focused sampling strategy that can isolate SSA from continental dust and anthropogenic aerosols, it is not possible to precisely quantify the contribution of SSA to the total aerosol loading of TEs. However, we can speculate based on the influences previously discussed. In Figure 4, we plot the range of percentage SSA contributions to GP15 aerosol TEs based on measured aerosol Na concentrations and the following four scenarios:

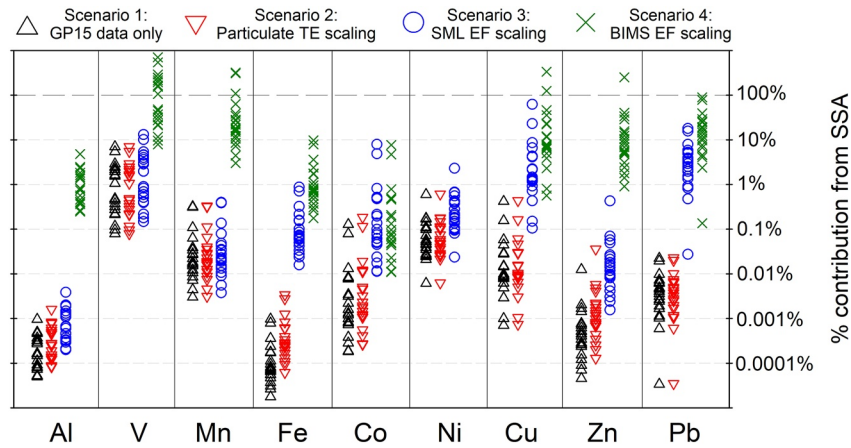

Figure 4. Percentage contributions from sea spray aerosol to GP15 aerosol trace element (TE) concentrations calculated using aerosol Na concentrations and towfish dissolved TE/Na ratios only (Scenario 1; black triangles) and with different scaling factors applied to the resulting data: red-inverted triangles—Scenario 2, scaled to account for particulate TE contributions; blue circles—Scenario 3, scaled using maximum surface microlayer enrichments from Table 6; green crosses—Scenario 4, scaled using enrichment factors from Weisel, Duce, Fasching, et al. (1984) Bubble Interfacial Microlayer Sampler (BIMS) data. For each scenario, individual data points are based upon individual aerosol samples collected along the section.

Scenario (1): TE/Na ratios of SSA are directly related to the concentrations of dissolved elements in near-surface seawater (assessed using GP15 towfish data);

Scenario (2): As for the first scenario, but also accounting for potential incorporation of particulate material into SSA by applying a scaling factor of the particulate/dissolved TE concentration ratio (assessed using average values from GP16 towfish data; Table 4);

Scenario (3): The TE content of SSA is driven by enrichments of TEs within the surface microlayer; here, we apply to our towfish TE/Na data the maximum observed SML EFs taken from the literature cited in Table 6;

Scenario (4): The TE content of SSA during GP15 is driven by the bubble-induced enrichments measured by Weisel, Duce, Fasching, et al. (1984); for this scenario, we use the EFs summarized in Table 4 of that paper and represented in our Table 5.

Figure 4 highlights that if the SSA TE/Na ratio is representative of bulk surface seawater (Scenario 1), its contribution to the total aerosol TE loading during GP15 would be <1% for all elements except V, regardless of whether a scaling factor to account for particulate TE concentrations is used (Scenario 2). Consideration of enrichments measured in SML and SSA samples (Scenarios 3 and 4), relative to bulk seawater, changes this interpretation in different ways for different elements as discussed below.

4.5.1. Vanadium

Of the elements considered here, V was calculated as having the highest SSA contribution to total aerosol loading (averaging 1.5%) based solely on surface seawater dissolved TE concentrations (Scenario 1). This may be partly due to the order of magnitude higher concentrations of dissolved V in surface seawater relative to the other elements (Table 2). The aerosol V distribution during GP15 had a distinct decrease in concentrations between the North Pacific and equatorial Pacific (Figure 3), which has been attributed to reduced influence from fuel combustion emissions as well as lower mineral aerosol loading during the southern part of the transect (Marsay et al., 2022). This results in significantly higher percentage contributions of V from SSA for equatorial Pacific samples (Aer13–Aer23; Figure 3) despite a slightly lower average sea salt aerosol concentration in this region (Figure 2).

Due to the dominance of the dissolved fraction of V in seawater (Ho et al., 2018), application of a scaling factor for particulate V (Scenario 2) had little influence on the range of SSA percentages, while the very limited number of V measurements in SML samples indicate enrichment of a factor of two or less based on total V concentrations. Application of the SSA EF calculated by Weisel, Duce, Fasching, et al. (1984) (Scenario 4) results in a significant increase in the calculated SSA contribution to aerosol V with 11 of the 21 values being >100%. This is clearly

an overestimate of the SSA contribution and may be partly explained by the BIMS-derived EF representing an upper estimate due to many of their V concentrations being below the detection limit (Weisel, Duce, Fasching, et al., 1984). Nevertheless, given the relatively high percentage contribution of SSA to total aerosol V concentrations calculated solely from towfish V/Na ratios in this study, it is clear that any significant enrichment (e.g., an EF of 10 or more) of V during the SSA production could result in it representing a substantial contribution to aerosol V loading in some regions; for example, during Leg 2 of GP15.

4.5.2. Aluminum, Manganese, Nickel, and Zinc

Based on seawater TE/Na ratios and aerosol Na measurements, these four elements had varying but insignificant contributions from SSA to their total aerosol loading (Scenario 1), even when accounting for particulate TE concentrations (Scenario 2). The particularly low contributions calculated for Al (<0.002%) are likely due to it being a major component of crustal material (~8% by weight, on average (Taylor & McLennan, 1995)), such that any mineral aerosol present would heavily influence aerosol Al. The low contribution of SSA Zn calculated from towfish data possibly reflects its approximately order of magnitude lower concentrations in oligotrophic surface seawater than the other three elements (Table 2).

Of these four elements, reported SML enrichments relative to bulk seawater for Al, Mn, and Ni have been low (EF < 5, based on maximum values from limited studies; Table 6), while reported SML EFs for Zn have reached 34 for the Mediterranean Sea (Tovar-Sánchez et al., 2020). However, for our data set, Ni is the only one of these four elements for which the application of the SML EF pushes the calculated SSA contribution above 1% for any samples, and this is for Aer04 only, which had the highest sea salt loading (Figure 2) and a low aerosol Ni concentration (Marsay et al., 2022).

No BIMS enrichment data are available for Ni, but for Al, Mn, and Zn enrichments reported by Weisel, Duce, Fasching, et al. (1984) are at least 100 times higher than the highest reported SML enrichments. For Mn, this EF (1,000) is enough to increase the calculated SSA contribution to >100% for three samples with other samples ranging from 3% to 64%. However, as for V, Weisel and coauthors noted that their EF value for Mn represents an upper estimate due to Mn being below the detection limit in several samples. For Al, applying the BIMS-derived average EF (5,000) gives SSA contributions ranging from 0.2% to 4.8%. This is slightly lower than the SSA contributions to Al of 10%–20% calculated for the western North Atlantic during the low dust season (Arimoto et al., 2003), which were also based on observed aerosol Na concentrations and the Al/Na ratio from the BIMS-collected samples. However, as for the other elements considered here, the lack of other such data sets makes it difficult to assess whether the Sargasso Sea enrichments are applicable to SSA produced in the Pacific Ocean.

Zinc had the highest average BIMS-derived EF of these four elements at 20,000. Applying this to our GP15 data is enough to increase the average SSA contribution to 23%, which is also comparable to the average calculated for SSA contribution to Zn at Bermuda (30 ± 22%) by Arimoto et al. (2003), based on the BIMS-derived SSA Zn/Na ratio. As for V and Mn, however, it is questionable whether the Sargasso Sea BIMS data are applicable to the Pacific Ocean with one calculated SSA contribution (Aer04) being as high as 165%. It is also noteworthy that other calculated EFs for Zn in SSA are much lower than that from the Sargasso Sea study (Pattenden et al., 1981; Piotrowicz et al., 1979; van Grieken et al., 1974) and closer to the maximum SML enrichment listed in Table 6. If we instead apply the much lower BIMS-derived EF of 230 that was determined from sampling in Narragansett Bay (Piotrowicz et al., 1979), the maximum SSA contribution to aerosol Zn along the GP15 transect would be just 2.9% with an average of 0.3%.

4.5.3. Cobalt

SSA Co contributions calculated from GP15 towfish data (Scenario 1) covered the largest spread in values due to Co having the greatest relative range in surface seawater concentrations (Figure 4, Table 2), but the contributions were always <0.2%, for both Scenario 1 and Scenario 2. In what may simply be a coincidence from having a limited number of studies to compare, Co was unique among the elements considered in that the maximum EF reported from SML studies was approximately the same as the enrichment reported for BIMS-derived aerosols. After applying either of these EFs, two samples that had among the lowest mineral aerosol loading during GP15 (Aer03 and Aer04; Figure 2) had SSA contributions of 4%–8% with the remaining samples having a <1% contribution.

4.5.4. Iron, Copper, and Lead

For Fe, Cu, and Pb, maximum reported SML EFs were approximately within an order of magnitude of the EFs reported for Sargasso Sea BIMS-generated aerosols (Tables 5 and 6). Of these three elements, Fe had the lowest calculated SSA contribution based solely on towfish data (Scenario 1). As described previously for Al, this is likely primarily due to it being a relatively major component of lithogenic material, thus being strongly influenced by any mineral aerosol present, coupled with the low solubility of Fe in seawater and the strong biological uptake of Fe in oligotrophic surface waters. The three elements are grouped together here because, for each, SML EFs of >100 were applied. Again, it should be emphasized that the maximum scaling factors derived from microlayer studies have been applied, and there have been other SML measurements of these elements that have indicated EFs of <10 (Table 6).

In the case of Fe, the mineral aerosol contribution is so dominant that even after applying the maximum reported SML EF, the calculated SSA contribution during GP15 is still always <1%. If instead the BIMS-derived EF of 10,000 is applied, the potential SSA contribution reaches 10% (for Aer04) but averages ~2% across the section. This value is similar to the calculated SSA contribution to aerosol Fe at Bermuda during periods of low dust loading (Arimoto et al., 2003), which also used the Sargasso Sea BIMS-derived data to calculate SSA contributions. For Cu and Pb, applying the maximum SML EF increases median SSA contributions to ~2%, and as high as 62% (Cu) and 18% (Pb) for Aer04, while the use of BIMS-derived EFs pushes median SSA contributions up to 7% (Cu) and 13% (Pb) with Aer03 and Aer04 samples both having SSA Cu of >100%. Again, this indicates that at least for Cu, the BIMS-generated SSA enrichments are not universally applicable.

The separation of truly "marine-derived" SSA contributions to the total aerosol TE load from recycled mineral aerosol particles is difficult to accomplish even with targeted sampling. This may in part account for some of the high EFs calculated during the Sargasso Sea BIMS study. In that case, the authors mostly used surface ocean TE concentrations measured during the same research cruise (with the exceptions of Fe and Co) to calculate marine aerosol EFs (Weisel, Duce, Fasching, et al., 1984). Although unfiltered seawater samples were collected for those measurements, the extraction and analytical methods used (Bruland & Franks, 1983; Weisel, Duce, & Fasching, 1984) did not include any digestion with strong acids, which could potentially have resulted in underestimated contributions from refractory particulate material (i.e., recently deposited mineral aerosol particles) in surface seawater. If this was the case, the calculated EFs would represent overestimates due to the potential for some of the SSA loading to be contributed by recycled mineral aerosol. This is particularly relevant given that the BIMS study took place during the summer, when Saharan dust transport to the region is greatest, with the elements most likely to be affected by this being the lithogenic elements of Fe, Al, and potentially Co and Mn.

Another aspect of the SSA contribution to aerosol TE loading is that mineral aerosol concentrations over the open ocean vary to a much greater extent than do sea salt concentrations. Although dust concentrations during GP15 were relatively low, averaging <100 ng/m^3, previous studies have reported average concentrations an order of magnitude lower, for example, in the South Pacific (Arimoto et al., 1987; Wagener et al., 2008). In such cases, it would be expected that SSA makes a more significant contribution to aerosol TE loading, assuming that surface seawater TE concentrations do not change as sharply as aerosol concentrations. Conversely, during the springtime maximum in dust and anthropogenic aerosol transport across the North Pacific from Asia, SSA contributions to total aerosol TE loading would become much less significant than those calculated here. This temporal variation in the significance of an SSA contribution to aerosol TEs has been discussed by Arimoto et al. (2003) with regard to Saharan dust transport to Bermuda.

5. Conclusions

While direct measurements of TE concentrations in fresh SSA were beyond the scope of this study, the combination of low dust loading during GP15 and the coincident TE measurements in aerosols and surface ocean samples has allowed us to revisit a poorly constrained aspect of TE biogeochemistry, namely, the relative contribution of SSA to aerosol TE loading.

Calculations based on surface seawater TE concentrations and aerosol Na measurements suggest negligible contributions of <1% for all elements considered except V, for which the SSA contribution averaged 1.5% and reached 7%. However, this calculation excludes the potential enrichment, relative to bulk seawater, of TEs during

SSA production, which has been suggested by a small number of ship-based and laboratory studies. If we apply EFs derived from the most comprehensive such study carried out in open ocean waters, we find that SSA could contribute significantly to aerosol TE loading for some elements. However, our data also reveal that a general application of this BIMS-derived data may not be appropriate. This conclusion is supported by measured enrichments of TEs in surface microlayer samples and from a handful of similar SSA-focused studies generally being very much lower than those from the Sargasso Sea study. We suggest that further focused measurements of TE enrichments in SSA will be useful to better understand its contribution to aerosol TE loading.

Given that in our assessment we use aerosol TE concentrations from a low-mineral aerosol loading season, we suggest that SSA contributions to some aerosol TEs (notably Fe, Al, and Co) are insignificant on a global basis. However, this does not preclude that, under low dust loading conditions found in certain ocean regions and at certain times of year, the SSA contribution could represent a small but significant fraction. For some other elements considered here, notably V, Cu, and Pb, the SSA contribution could be more important, though there is considerable uncertainty that warrants further study. In cases where the SSA contribution to total aerosol TE loading is significant, not accounting for it when calculating deposition fluxes from measured bulk aerosol TE concentration data sets would result in an overestimation of the atmospheric supply of continental materials (including lithogenic, anthropogenic, and volcanic emissions) to the surface ocean.

Data Availability Statement

The data used in this study include chemical concentration data from discrete aerosol and seawater samples. The total aerosol trace element data (Buck et al., 2021a, 2021b) and soluble aerosol sodium data (Buck et al., 2022a, 2022b) are archived at the Biological and Chemical Oceanography Data Management Office (BCO-DMO). The dissolved cobalt, dissolved aluminum, dissolved manganese, dissolved nickel, and dissolved lead concentration data from surface seawater samples are archived at BCO-DMO as well (Freiberger et al., 2022a, 2022b; Hatta & Measures, 2022a, 2022b; M. A. Saito, 2021; M. Saito, 2020). Surface seawater data for dissolved iron, dissolved copper, dissolved zinc, and dissolved vanadium are submitted to BCO-DMO but have not yet been published as of the time of this submission. These data are available in Table S1 of this work for purposes of peer review. Data archived at BCO-DMO are licensed under Creative Commons Attribution 4.0.

Acknowledgments
This research was supported by the National Science Foundation (NSF) grants OCE-1756103 to C. S. Buck, OCE-1756104 to W. M. Landing, OCE-1737024 to A.M. Shiller, OCE-1736906 to M. Hatta, OCE-1736875 to C. P. Till, OCE-1737167 to J. N. Fitzsimmons, and OCE-1736599 to M. Saito. In addition, N. T. Lanning was supported by the NSF Graduate Research Fellowship Program award 1746932. The authors gratefully acknowledge Sveinn Einarsson and Kyle McQuiggan for towfish deployment, recovery and maintenance, Laramie Jensen and Brent Summers for overseeing acidification and distribution of towfish samples, the Oceanographic Data Facility team from Scripps Institution of Oceanography for salinity measurements, the captain and crew of the R/V Roger Revelle for their support during U.S. GEOTRACES GP15, and the work of Chief Scientists Phoebe Lam, Karen Casciotti, and Greg Cutter.

References

Achterberg, E. P., Moore, C. M., Henson, S. A., Steigenberger, S., Stohl, A., Eckhardt, S., et al. (2013). Natural iron fertilization by the Eyjafjallajökull volcanic eruption. *Geophysical Research Letters*, *40*(5), 921–926. https://doi.org/10.1002/grl.50221

Aller, J. Y., Kuznetsova, M. R., Jahns, C. J., & Kemp, P. F. (2005). The sea surface microlayer as a source of viral and bacterial enrichment in marine aerosols. *Journal of Aerosol Science*, *36*(5–6), 801–812. https://doi.org/10.1016/j.jaerosci.2004.10.012

Arimoto, R., Duce, R. A., Ray, B. J., Ellis, W. G., Jr., Cullen, J. D., & Merrill, J. T. (1995). Trace elements in the atmosphere over the North Atlantic. *Journal of Geophysical Research*, *100*(D1), 1199–1213. https://doi.org/10.1029/94JD02618

Arimoto, R., Duce, R. A., Ray, B. J., Hewitt, A. D., & Williams, J. (1987). Trace elements in the atmosphere of American Samoa: Concentrations and deposition to the tropical South Pacific. *Journal of Geophysical Research*, *92*(D7), 8465–8479. https://doi.org/10.1029/JD092iD07p08465

Arimoto, R., Duce, R. A., Ray, B. J., & Tomza, U. (2003). Dry deposition of trace elements to the western North Atlantic. *Global Biogeochemical Cycles*, *17*(1), 1010. https://doi.org/10.1029/2001GB001406

Barker, D. R., & Zeitlin, H. (1972). Metal-ion concentrations in sea-surface microlayer and size-separated atmospheric aerosol samples in Hawaii. *Journal of Geophysical Research*, *77*(27), 5076–5086. https://doi.org/10.1029/JC077i027p05076

Biller, D. V., & Bruland, K. W. (2012). Analysis of Mn, Fe, Co, Ni, Cu, Zn, Cd, and Pb in seawater using the Nobias-chelate PA1 resin and magnetic sector inductively coupled plasma mass spectrometry (ICP-MS). *Marine Chemistry*, *130–131*, 12–20. https://doi.org/10.1016/j.marchem.2011.12.001

Blanchard, D. C. (1989). The ejection of drops from the sea and their enrichment with bacteria and other materials: A review. *Estuaries*, *12*(3), 127–137. https://doi.org/10.2307/1351816

Blanchard, D. C., & Syzdek, L. (1970). Mechanism for the water-to-air transfer and concentration of bacteria. *Science*, *170*(3958), 626–628. https://doi.org/10.1126/science.170.3958.626

Boiteau, R. M., Till, C. P., Ruacho, A., Bundy, R. M., Hawco, N. J., McKenna, A. M., et al. (2016). Structural characterization of natural nickel and copper binding ligands along the US GEOTRACES Eastern Pacific Zonal Transect. *Frontiers in Marine Science*, *3*, 243. https://doi.org/10.3389/fmars.2016.00243

Boucher, O., Randall, D., Artaxo, P., Bretherton, C., Feingold, G., Forster, P., et al. (2013). Clouds and aerosols. In T. F. Stocker, D. Qin, G.-K. Plattner, M. Tignor, S. K. Allen, J. Boschung, et al. (Eds.), *Climate Change 2013: The Physical Science Basis. Contribution of Working Group I to the Fifth Assessment Report of the Intergovernmental Panel on Climate Change* (pp. 571–657). Cambridge University Press.

Boyle, E. A., Zurbrick, C., Lee, J.-M., Till, R., Till, C. P., Zhang, J., & Flegal, A. R. (2020). Lead and lead isotopes in the U.S. GEOTRACES East Pacific Zonal Transect (GEOTRACES GP16). *Marine Chemistry*, *227*, 103892. https://doi.org/10.1016/j.marchem.2020.103892

Bruland, K. W., & Franks, R. P. (1983). Mn, Ni, Cu, Zn and Cd in the western North Atlantic. In C. S. Wong, E. Boyle, K. W. Bruland, J. D. Burton, & E. D. Goldberg (Eds.) *Trace Metals in Sea Water. NATO Conference Series (IV Marine Sciences)* (Vol. 9, pp. 395–414). Springer.

Bruland, K. W., Rue, E. L., Smith, G. J., & DiTullio, G. R. (2005). Iron, macronutrients and diatom blooms in the Peru upwelling regime: Brown and blue waters of Peru. *Marine Chemistry*, *93*(2–4), 81–103. https://doi.org/10.1016/j.marchem.2004.06.011

Buck, C. S., Landing, W. M., & Marsay, C. (2022a). Concentrations of deionized water-soluble aerosol major ions from bulk aerosol samples collected on Leg 1 (Seattle, WA to Hilo, HI) of the US GEOTRACES Pacific Meridional Transect (PMT) cruise (GP15, RR1814) on R/V Roger Revelle from Sept-Oct 2018. Biological and Chemical Oceanography Data Management Office (BCO-DMO). (Version 1) Version Date 2022-06-21. Retrieved from http://lod.bco-dmo.org/id/dataset/875955

Buck, C. S., Landing, W. M., & Marsay, C. (2022b). Concentrations of deionized water-soluble aerosol major ions from bulk aerosol samples collected on Leg 2 (Hilo, HI to Papeete, French Polynesia) of the US GEOTRACES PMT cruise (GP15, RR1815) on R/V Roger Revelle from Oct-Nov 2018. Biological and Chemical Oceanography Data Management Office (BCO-DMO). (Version 1) Version Date 2022-06-21. Retrieved from http://lod.bco-dmo.org/id/dataset/876005

Buck, C. S., Landing, W. M., Resing, J. A., & Lebon, G. T. (2006). Aerosol iron and aluminum solubility in the northwest Pacific Ocean: Results from the 2002 IOC cruise. *Geochemistry, Geophys. Geosystems*, *7*(4), Q04M07. https://doi.org/10.1029/2005GC000977

Buck, C. S., Marsay, C., & Landing, W. M. (2021a). Total aerosol trace elements from bulk aerosol samples collected on Leg 1 (Seattle, WA to Hilo, HI) of the US GEOTRACES Pacific Meridional Transect (PMT) cruise (GP15, RR1814) on R/V Roger Revelle from September to October 2018. Biological and Chemical Oceanography Data Management Office (BCO-DMO). (Version 1) Version Date 2020-12-17. https://doi.org/10.26008/1912/bco-dmo.834230.1

Buck, C. S., Marsay, C., & Landing, W. M. (2021b). Total aerosol trace elements from bulk aerosol samples collected on Leg 2 (Hilo, HI to Papeete, French Polynesia) of the US GEOTRACES Pacific Meridional Transect (PMT) cruise (GP15, RR1815) on R/V Roger Revelle from Oct-Nov 2018. Biological and Chemical Oceanography Data Management Office (BCO-DMO). (Version 1) Version Date 2020-12-18. https://doi.org/10.26008/1912/bco-dmo.834243.1

Cattell, F. C. R., & Scott, W. D. (1978). Copper in aerosol particles produced by the ocean. *Science*, *202*(4366), 429–430. https://doi.org/10.1126/science.202.4366.429

Cavalli, F., Facchini, M. C., Decesari, S., Mircea, M., Emblico, L., Fuzzi, S., et al. (2004). Advances in characterization of size-resolved organic matter in marine aerosol over the North Atlantic. *Journal of Geophysical Research*, *109*(24), D24215. https://doi.org/10.1029/2004JD005137

Chmiel, R., Lanning, N., Laubach, A., Lee, J. M., Fitzsimmons, J., Hatta, M., et al. (2022). Major processes of the dissolved cobalt cycle in the North and equatorial Pacific Ocean. *Biogeosciences*, *19*(9), 2365–2395. https://doi.org/10.5194/bg-19-2365-2022

Cunliffe, M., Engel, A., Frka, S., Gašparović, B. Ž., Guitart, C., Murrell, J. C., et al. (2013). Sea surface microlayers: A unified physicochemical and biological perspective of the air-ocean interface. *Progress in Oceanography*, *109*, 104–116. https://doi.org/10.1016/j.pocean.2012.08.004

Cutter, G., Casciotti, K., Croot, P., Geibert, W., Heimbürger, L.-E., Lohan, M., et al. (2017). Sampling and sample-handling protocols for GEOTRACES Cruises, Version 3.0 (p. 178). Retrieved from https://www.geotraces.org/methods-cookbook/

de Leeuw, G., Andreas, E. L., Anguelova, M. D., Fairall, C. W., Lewis, E. R., O'Dowd, C., et al. (2011). Production flux of sea spray aerosol. *Reviews of Geophysics*, *49*(2), RG2001. https://doi.org/10.1029/2010RG000349

Desboeufs, K. V., Sofikitis, A., Losno, R., Colin, J. L., & Ausset, P. (2005). Dissolution and solubility of trace metals from natural and anthropogenic aerosol particulate matter. *Chemosphere*, *58*(2), 195–203. https://doi.org/10.1016/j.chemosphere.2004.02.025

Duce, R. A., Arimoto, R., Ray, B. J., Unni, C. K., & Harder, P. J. (1983). Atmospheric trace elements at Enewetak Atoll: 1. Concentrations, sources, and temporal variability. *Journal of Geophysical Research*, *88*(C9), 5321–5342. https://doi.org/10.1029/JC088iC09p05321

Duce, R. A., & Hoffman, E. J. (1976). Chemical fractionation at the air/sea interface. *Annual Review of Earth and Planetary Sciences*, *4*(1), 187–228. https://doi.org/10.1146/annurev.ea.04.050176.001155

Duce, R. A., Quinn, J. G., Olney, C. E., Piotrowicz, S. R., Ray, B. J., & Wade, T. L. (1972). Enrichment of heavy metals and organic compounds in the surface microlayer of Narragansett Bay, Rhode Island. *Science*, *176*(4031), 161–163. https://doi.org/10.1126/science.176.4031.161

Duce, R. A., Unni, C. K., Ray, B. J., Prospero, J. M., & Merrill, J. T. (1980). Long-range atmospheric transport of soil dust from Asia to the tropical North Pacific: Temporal variability. *Science*, *209*(4464), 1522–1524. https://doi.org/10.1126/science.209.4464.1522

Ebling, A. M., & Landing, W. M. (2015). Sampling and analysis of the sea surface microlayer for dissolved and particulate trace elements. *Marine Chemistry*, *177*, 134–142. https://doi.org/10.1016/j.marchem.2015.03.012

Ebling, A. M., & Landing, W. M. (2017). Trace elements in the sea surface microlayer: Rapid responses to changes in aerosol deposition. *Elementa: Science of the Anthropocene*, *5*, 42. https://doi.org/10.1525/elementa.237

Freiberger, R., Fitzsimmons, J. N., & Till, C. P. (2022a). Surface fish dissolved metals (Ni, Mn, Pb, Ce, Y, La) from Leg 1 (Seattle, WA to Hilo, HI) of the US GEOTRACES Pacific Meridional Transect (PMT) cruise (GP15, RR1814) on R/V Roger Revelle from September to Octobe 2018 (Version 1) [Dataset]. Biological and Chemical Oceanography Data Management Office (BCO-DMO). https://doi.org/10.26008/1912/bco-dmo.876536.1

Freiberger, R., Fitzsimmons, J. N., & Till, C. P. (2022b). Surface fish dissolved metals (Ni, Mn, Pb, Ce, Y, La) from Leg 2 (Hilo, HI to Papeete, French Polynesia) of the US GEOTRACES PMT cruise (GP15, RR1815) on R/V Roger Revelle from Oct-Nov 2018 (Version 1) [Dataset]. Biological and Chemical Oceanography Data Management Office (BCO-DMO). https://doi.org/10.26008/1912/bco-dmo.876550.1

Guasco, T. L., Cuadra-Rodriguez, L. A., Pedler, B. E., Ault, A. P., Collins, D. B., Zhao, D., et al. (2014). Transition metal associations with primary biological particles in sea spray aerosol generated in a wave channel. *Environmental Science & Technology*, *48*(2), 1324–1333. https://doi.org/10.1021/es403203d

Hamilton, D. S., Moore, J. K., Arneth, A., Bond, T. C., Carslaw, K. S., Hantson, S., et al. (2020). Impact of changes to the atmospheric soluble iron deposition flux on ocean biogeochemical cycles in the Anthropocene. *Global Biogeochemical Cycles*, *34*(3), e2019GB006448. https://doi.org/10.1029/2019GB006448

Hardy, J. T. (1982). The sea surface microlayer: Biology, chemistry and anthropogenic enrichment. *Progress in Oceanography*, *11*(4), 307–328. https://doi.org/10.1016/0079-6611(82)90001-5

Hathorne, E. C., Haley, B., Stichel, T., Grasse, P., Zieringer, M., & Frank, M. (2012). Online preconcentration ICP-MS analysis of rare Earth elements in seawater. *Geochemistry, Geophysics, Geosystems*, *13*(1), Q01020. https://doi.org/10.1029/2011GC003907

Hatta, M., & Measures, C. I. (2022a). Shipboard FIA of Dissolved Al, Fe, and Mn from Leg 1 (Seattle, WA to Hilo, HI) of the US GEOTRACES Pacific Meridional Transect (PMT) cruise (GP15, RR1814) on R/V Roger Revelle from September to October 2018. Biological and Chemical Oceanography Data Management Office (BCO-DMO). (Version 1) Version Date 2022-06-27. https://doi.org/10.26008/1912/bco-dmo.876137.1

Hatta, M., & Measures, C. I. (2022b). Shipboard FIA of Dissolved Al, Fe, and Mn from Leg 2 (Hilo, HI to Papeete, French Polynesia) of the US GEOTRACES Pacific Meridional Transect (PMT) cruise (GP15, RR1815) on R/V Roger Revelle from October to November 2018. Biological and Chemical Oceanography Data Management Office (BCO-DMO). (Version 1) Version Date 2022-06-27. https://doi.org/10.26008/1912/bco-dmo.876152.1

Hawco, N. J., Ohnemus, D. C., Resing, J. A., Twining, B. S., & Saito, M. A. (2016). A dissolved cobalt plume in the oxygen minimum zone of the eastern tropical South Pacific. *Biogeosciences*, *13*(20), 5697–5717. https://doi.org/10.5194/bg-13-5697-2016

Ho, P., Lee, J.-M., Heller, M. I., Lam, P. J., & Shiller, A. M. (2018). The distribution of dissolved and particulate Mo and V along the U.S. GEOTRACES East Pacific Zonal Transect (GP16): The roles of oxides and biogenic particles in their distributions in the oxygen deficient zone and the hydrothermal plume. *Marine Chemistry*, *201*, 242–255. https://doi.org/10.1016/j.marchem.2017.12.003

Ho, P., Resing, J. A., & Shiller, A. M. (2019). Processes controlling the distribution of dissolved Al and Ga along the U.S. GEOTRACES East Pacific Zonal Transect (GP16). *Deep Sea Research Part I: Oceanographic Research Papers*, *147*, 128–145. https://doi.org/10.1016/j.dsr.2019.04.009

Hsu, S.-C., Liu, S. C., Huang, Y.-T., Lung, S.-C. C., Tsai, F., Tu, J.-Y., & Kao, S.-J. (2008). A criterion for identifying Asian dust events based on Al concentration data collected from northern Taiwan between 2002 and early 2007. *Journal of Geophysical Research*, *113*(D18), D18306. https://doi.org/10.1029/2007JD009574

Ito, A., Myriokefalitakis, S., Kanakidou, M., Mahowald, N. M., Scanza, R. A., Hamilton, D. S., et al. (2019). Pyrogenic iron: The missing link to high iron solubility in aerosols. *Science Advances*, *5*(5), eaau7671. https://doi.org/10.1126/sciadv.aau7671

Jayarathne, T., Sultana, C. M., Lee, C., Malfatti, F., Cox, J. L., Pendergraft, M. A., et al. (2016). Enrichment of saccharides and divalent cations in sea spray aerosol during two phytoplankton blooms. *Environmental Science & Technology*, *50*(21), 11511–11520. https://doi.org/10.1021/acs.est.6b02988

Jensen, L. T., Wyatt, N. J., Landing, W. M., & Fitzsimmons, J. N. (2020). Assessment of the stability, sorption, and exchangeability of marine dissolved and colloidal metals. *Marine Chemistry*, *220*, 103754. https://doi.org/10.1016/j.marchem.2020.103754

Jickells, T. D., An, Z. S., Andersen, K. K., Baker, A. R., Bergametti, G., Brooks, N., et al. (2005). Global iron connections between desert dust, ocean biogeochemistry, and climate. *Science*, *308*(5718), 67–71. https://doi.org/10.1126/science.1105959

John, S. G., Helgoe, J., & Townsend, E. (2018). Biogeochemical cycling of Zn and Cd and their stable isotopes in the Eastern Tropical South Pacific. *Marine Chemistry*, *201*, 256–262. https://doi.org/10.1016/j.marchem.2017.06.001

Kaufman, Y. J., Koren, I., Remer, L. A., Tanré, D., Ginoux, P., & Fan, S. (2005). Dust transport and deposition observed from the Terra-Moderate Resolution Imaging Spectroradiometer (MODIS) spacecraft over the Atlantic Ocean. *Journal of Geophysical Research*, *110*(D10), D10S12. https://doi.org/10.1029/2003JD004436

Keene, W. C., Maring, H., Maben, J. R., Kieber, D. J., Pszenny, A. A. P., Dahl, E. E., et al. (2007). Chemical and physical characteristics of nascent aerosols produced by bursting bubbles at a model air-sea interface. *Journal of Geophysical Research*, *112*(21), D21202. https://doi.org/10.1029/2007JD008464

Lagerström, M. E., Field, M. P., Séguret, M., Fischer, L., Hann, S., & Sherrell, R. M. (2013). Automated on-line flow-injection ICP-MS determination of trace metals (Mn, Fe, Co, Ni, Cu and Zn) in open ocean seawater: Application to the GEOTRACES program. *Marine Chemistry*, *155*, 71–80. https://doi.org/10.1016/j.marchem.2013.06.001

Langmann, B., Zakšek, K., Hort, M., & Duggen, S. (2010). Volcanic ash as fertiliser for the surface ocean. *Atmospheric Chemistry and Physics*, *10*(8), 3891–3899. https://doi.org/10.5194/acp-10-3891-2010

Mahowald, N. M., Artaxo, P., Baker, A. R., Jickells, T. D., Okin, G. S., Randerson, J. T., & Townsend, A. R. (2005). Impacts of biomass burning emissions and land use change on Amazonian atmospheric phosphorus cycling and deposition. *Global Biogeochemical Cycles*, *19*(4), GB4030. https://doi.org/10.1029/2005GB002541

Mahowald, N. M., Engelstaedter, S., Luo, C., Sealy, A., Artaxo, P., Benitez-Nelson, C., et al. (2009). Atmospheric iron deposition: Global distribution, variability, and human perturbations. *Annual Review of Marine Science*, *1*, 245–278. https://doi.org/10.1146/annurev.marine.010908.163727

Mahowald, N. M., Hamilton, D. S., Mackey, K. R. M., Moore, J. K., Baker, A. R., Scanza, R. A., & Zhang, Y. (2018). Aerosol trace metal leaching and impacts on marine microorganisms. *Nature Communications*, *9*(1), 2614. https://doi.org/10.1038/s41467-018-04970-7

Mahowald, N. M., Scanza, R., Brahney, J., Goodale, C. L., Hess, P. G., Moore, J. K., & Neff, J. (2017). Aerosol deposition impacts on land and ocean carbon cycles. *Current Climate Change Reports*, *3*(1), 16–31. https://doi.org/10.1007/s40641-017-0056-z

Marsay, C. M., Kadko, D., Landing, W. M., & Buck, C. S. (2022). Bulk aerosol trace element concentrations and deposition fluxes during the U.S. GEOTRACES GP15 Pacific Meridional Transect. *Global Biogeochemical Cycles*, *36*(2), e2021GB007122. https://doi.org/10.1029/2021GB007122

Martin, J. H., Fitzwater, S. E., & Gordon, R. M. (1990). Iron deficiency limits phytoplankton growth in Antarctic waters. *Global Biogeochemical Cycles*, *4*(1), 5–12. https://doi.org/10.1029/GB004i001p00005

Merrill, J. T., Uematsu, M., & Bleck, R. (1989). Meteorological analysis of long range transport of mineral aerosols over the North Pacific. *Journal of Geophysical Research*, *94*(D6), 8584–8598. https://doi.org/10.1029/JD094iD06p08584

Moore, C. M., Mills, M. M., Arrigo, K. R., Berman-Frank, I., Bopp, L., Boyd, P. W., et al. (2013). Processes and patterns of oceanic nutrient limitation. *Nature Geoscience*, *6*(9), 701–710. https://doi.org/10.1038/ngeo1765

Moore, J. K., Doney, S. C., & Lindsay, K. (2004). Upper ocean ecosystem dynamics and iron cycling in a global three-dimensional model. *Global Biogeochemical Cycles*, *18*(4), GB4028. https://doi.org/10.1029/2004GB002220

O'Dowd, C. D., Facchini, M. C., Cavalli, F., Ceburnis, D., Mircea, M., Decesari, S., et al. (2004). Biogenically driven organic contribution to marine aerosol. *Nature*, *431*(7009), 676–680. https://doi.org/10.1038/nature02959

Pacyna, J. M., Sundseth, K., & Pacyna, E. G. (2016). Sources and fluxes of harmful metals. In J. M. Pacyna & E. G. Pacyna (Eds.), *Environmental Determinants of Human Health* (pp. 1–25). Springer.

Parker, C. E., Brown, M. T., & Bruland, K. W. (2016). Scandium in the open ocean: A comparison with other group 3 trivalent metals. *Geophysical Research Letters*, *43*(6), 2758–2764. https://doi.org/10.1002/2016GL067827

Parrington, J. R., Zoller, W. H., & Aras, N. K. (1983). Asian dust: Seasonal transport to the Hawaiian Islands. *Science*, *220*(4593), 195–197. https://doi.org/10.1126/science.220.4593.195

Pattenden, N. J., Cambray, R. S., & Playford, K. (1981). Trace and major elements in the sea-surface microlayer. *Geochimica et Cosmochimica Acta*, *45*(1), 93–100. https://doi.org/10.1016/0016-7037(81)90266-0

Patterson, J. P., Collins, D. B., Michaud, J. M., Axson, J. L., Sultana, C. M., Moser, T., et al. (2016). Sea spray aerosol structure and composition using cryogenic transmission electron microscopy. *ACS Central Science*, *2*(1), 40–47. https://doi.org/10.1021/acscentsci.5b00344

Pilson, M. E. Q. (2013). *An introduction to the chemistry of the sea*. Cambridge University Press.

Pinedo-González, P., Hawco, N. J., Bundy, R. M., Armbrust, E. V., Follows, M. J., Cael, B. B., et al. (2020). Anthropogenic Asian aerosols provide Fe to the North Pacific Ocean. *Proceedings of the National Academy of Sciences of the United States of America*, *117*(45), 27862–27868. https://doi.org/10.1073/pnas.2010315117

Piotrowicz, S. R., Duce, R. A., Fasching, J. L., & Weisel, C. P. (1979). Bursting bubbles and their effect on the sea-to-air transport of Fe, Cu and Zn. *Marine Chemistry*, *7*(4), 307–324. https://doi.org/10.1016/0304-4203(79)90018-5

Prather, K. A., Bertram, T. H., Grassian, V. H., Deane, G. B., Stokes, M. D., DeMott, P. J., et al. (2013). Bringing the ocean into the laboratory to probe the chemical complexity of sea spray aerosol. *Proceedings of the National Academy of Sciences of the United States of America*, *110*(19), 7550–7555. https://doi.org/10.1073/pnas.1300262110

Prospero, J. M. (1979). Mineral and sea salt aerosol concentrations in various ocean regions. *Journal of Geophysical Research*, *84*(C2), 725–731. https://doi.org/10.1029/jc084ic02p00725

Prospero, J. M. (2002). The chemical and physical properties of marine aerosols: An introduction. In A. Gianguzza, E. Pelizzetti, & S. Sammartano (Eds.), *Chemistry of marine water and sediments* (pp. 35–82). Springer.

Prospero, J. M., Bullard, J. E., & Hodgkins, R. (2012). High-latitude dust over the North Atlantic: Inputs from Icelandic proglacial dust storms. *Science*, *335*(6072), 1078–1082. https://doi.org/10.1126/science.1217447

Prospero, J. M., Ginoux, P., Torres, O., Nicholson, S. E., & Gill, T. E. (2002). Environmental characterization of global sources of atmospheric soil dust identified with the Nimbus 7 Total Ozone Mapping Spectrometer (TOMS) absorbing aerosol product. *Reviews of Geophysics*, *40*(1), 1002–2-31. https://doi.org/10.1029/2000RG000095

Quinn, P. K., Bates, T. S., Schulz, K. S., Coffman, D. J., Frossard, A. A., Russell, L. M., et al. (2014). Contribution of sea surface carbon pool to organic matter enrichment in sea spray aerosol. *Nature Geoscience*, *7*(3), 228–232. https://doi.org/10.1038/ngeo2092

Resing, J. A., & Measures, C. I. (1994). Fluorometric determination of Al in seawater by flow injection analysis with in-line preconcentration. *Analytical Chemistry*, *66*(22), 4105–4111. https://doi.org/10.1021/ac00094a039

Resing, J. A., Sedwick, P. N., German, C. R., Jenkins, W. J., Moffett, J. W., Sohst, B. M., & Tagliabue, A. (2015). Basin-scale transport of hydrothermal dissolved metals across the South Pacific Ocean. *Nature*, *523*(7559), 200–203. https://doi.org/10.1038/nature14577

Robinson, T.-B., Giebel, H.-A., & Wurl, O. (2019). Riding the plumes: Characterizing bubble scavenging conditions for the enrichment of the sea-surface microlayer by transparent exopolymer particles. *Atmosphere*, *10*(8), 454. https://doi.org/10.3390/atmos10080454

Saito, M. (2020). Dissolved Cobalt and Labile Cobalt from Leg 2 (Hilo, HI to Papeete, French Polynesia) of the US GEOTRACES Pacific Meridional Transect (PMT) cruise (GP15, RR1815) on R/V Roger Revelle from October to November 2018. Biological and Chemical Oceanography Data Management Office (BCO-DMO). (Version 1) Version Date 2020-07-15 (if applicable, indicate subset used). https://doi.org/10.26008/1912/bco-dmo.818610.1

Saito, M. A. (2021). Dissolved Cobalt and Labile Cobalt from Leg 1 (Seattle, WA to Hilo, HI) of the US GEOTRACES Pacific Meridional Transect (PMT) cruise (GP15, RR1814) on R/V Roger Revelle from September to October 2018. Biological and Chemical Oceanography Data Management Office (BCO-DMO). (Version 2) Version Date 2021-05-05. https://doi.org/10.26008/1912/bco-dmo.818383.2

Saito, M. A., & Moffett, J. W. (2001). Complexation of cobalt by natural organic ligands in the Sargasso Sea as determined by a new high-sensitivity electrochemical cobalt speciation method suitable for open ocean work. *Marine Chemistry*, *75*(1–2), 49–68. https://doi.org/10.1016/S0304-4203(01)00025-1

Sedwick, P. N., Church, T. M., Bowie, A. R., Marsay, C. M., Ussher, S. J., Achilles, K. M., et al. (2005). Iron in the Sargasso Sea (Bermuda Atlantic Time-series Study region) during summer: Eolian imprint, spatiotemporal variability, and ecological implications. *Global Biogeochemical Cycles*, *19*(4), GB4006. https://doi.org/10.1029/2004GB002445

Shaw, G. E. (1995). The Arctic haze phenomenon. *Bulletin of the American Meteorological Society*, *76*(12), 2403–2413. https://doi.org/10.1175/1520-0477(1995)076<2403:TAHP>2.0.CO;2

Sherrell, R. M., Twining, B., & German, C. R. (2016). *Trace element concentrations in suspended particles collected from the GeoFISH during the R/V Thomas G. Thompson cruise TN303 from Peru to Tahiti in 2013 (U.S. GEOTRACES EPZT project)*. Biological and Chemical Oceanography Data Management Office (BCO-DMO). (Version Final. Version Date 2016-06-09). Retrieved from http://lod.bco-dmo.org/id/dataset/648543

Sholkovitz, E. R., Sedwick, P. N., & Church, T. M. (2009). Influence of anthropogenic combustion emissions on the deposition of soluble aerosol iron to the ocean: Empirical estimates for island sites in the North Atlantic. *Geochimica et Cosmochimica Acta*, *73*(14), 3981–4003. https://doi.org/10.1016/j.gca.2009.04.029

Sohrin, Y., Urushihara, S., Nakatsuka, S., Kono, T., Higo, E., Minami, T., et al. (2008). Multielemental determination of GEOTRACES key trace metals in seawater by ICPMS after preconcentration using an ethylenediaminetriacetic acid chelating resin. *Analytical Chemistry*, *80*(16), 6267–6273. https://doi.org/10.1021/ac800500f

Taylor, S. R., & McLennan, S. M. (1995). The geochemical evolution of the continental crust. *Reviews of Geophysics*, *33*(2), 241–265. https://doi.org/10.1029/95RG00262

Tovar-Sánchez, A., González-Ortegón, E., & Duarte, C. M. (2019). Trace metal partitioning in the top meter of the ocean. *Science of the Total Environment*, *652*, 907–914. https://doi.org/10.1016/j.scitotenv.2018.10.315

Tovar-Sánchez, A., Rodriguez-Romero, A., Engel, A., Zancker, B., Fu, F., Maranon, E., et al. (2020). Characterizing the surface microlayer in the Mediterranean Sea: Trace metal concentrations and microbial plankton abundance. *Biogeosciences*, *17*(8), 2349–2364. https://doi.org/10.5194/bg-17-2349-2020

van Grieken, R. E., Johansson, T. B., & Winchester, J. W. (1974). Trace metal fractionation effects between sea water and aerosols from bubble bursting. *Journal de Recherches Atmosphériques*, *8*, 611–621.

Wagener, T., Guieu, C., Losno, R., Bonnet, S., & Mahowald, N. (2008). Revisiting atmospheric dust export to the Southern Hemisphere ocean: Biogeochemical implications. *Global Biogeochemical Cycles*, *22*(2), GB2006. https://doi.org/10.1029/2007GB002984

Walker, M. I., Mckay, W. A., Pattenden, N. J., & Liss, P. S. (1986). Actinide enrichment in marine aerosols. *Nature*, *323*(6084), 141–143. https://doi.org/10.1038/323141a0

Wallace, G. T., & Duce, R. A. (1975). Concentration of particulate trace metals and particulate organic carbon in marine surface waters by a bubble flotation mechanism. *Marine Chemistry*, *3*(2), 157–181. https://doi.org/10.1016/0304-4203(75)90020-1

Weisel, C. P., Duce, R. A., & Fasching, J. L. (1984). Determination of aluminum, lead, and vanadium in North Atlantic seawater after coprecipitation with ferric hydroxide. *Analytical Chemistry*, *56*(6), 1050–1052. https://doi.org/10.1021/ac00270a044

Weisel, C. P., Duce, R. A., Fasching, J. L., & Heaton, R. W. (1984). Estimates of the transport of trace metals from the ocean to the atmosphere. *Journal of Geophysical Research*, *89*(D7), 11607–11618. https://doi.org/10.1029/JD089iD07p11607

Wurl, O., Wurl, E., Miller, L., Johnson, K., & Vagle, S. (2011). Formation and global distribution of sea-surface microlayers. *Biogeosciences*, *8*(1), 121–135. https://doi.org/10.5194/bg-8-121-2011

Zhang, X. Y., Arimoto, R., & An, Z. S. (1997). Dust emission from Chinese desert sources linked to variations in atmospheric circulation. *Journal of Geophysical Research*, *102*(23), 28041–28047. https://doi.org/10.1029/97jd02300